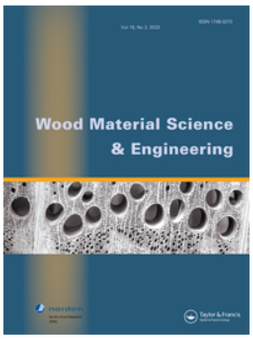

Wood Material Science & Engineering

ISSN: (Print) (Online) Journal homepage: https://www.tandfonline.com/loi/swoo20

Mode I fracture of beech-adhesive bondline at three different temperatures

Jaka Gašper Pečnik, Andreja Pondelak, Michael David Burnard & Václav Sebera

To cite this article: Jaka Gašper Pečnik, Andreja Pondelak, Michael David Burnard & Václav Sebera (2022): Mode I fracture of beech-adhesive bondline at three different temperatures, Wood Material Science & Engineering, DOI: 10.1080/17480272.2022.2135135

To link to this article: https://doi.org/10.1080/17480272.2022.2135135

WOOD MATERIAL SCIENCE & ENGINEERING
https://doi.org/10.1080/17480272.2022.2135135

Taylor & Francis
Taylor & Francis Group

ORIGINAL PAPER

Mode I fracture of beech-adhesive bondline at three different temperatures

Jaka Gašper Pečnik [a,b], Andreja Pondelak [c], Michael David Burnard [a,b] and Václav Sebera [d]

[a]InnoRenew CoE, Izola, Slovenia; [b]Andrej Marušič Institute, University of Primorska, Koper, Slovenia; [c]Slovenian National Building and Civil Engineering Institute, Ljubljana, Slovenia; [d]Department of Wood Science and Technology, Faculty of Forestry and Wood Technology, Mendel University in Brno, Brno, Czech

ABSTRACT

Single edge-notched three-point bending tests (SEN-TPB) for mode I were utilized to experimentally evaluate fracture properties of adhesive bondlines in European beech (*Fagus Sylvatica* L.). The bondline was examined at two anatomical planes with TR and RT orientation and at control and two elevated temperatures (70°C and 140°C). Among epoxy (EPI), melamine-urea formaldehyde (MUF), and polyurethane (PUR) adhesives, the highest average critical energy G_c with 0.80 N/mm and fracture energy G_f with 1079.4 N/mm were obtained for EPI in the TR plane and under standard climate conditions (20°C/65% relative humidity), followed by MUF ($G_c = 0.50$ N/mm and $G_f = 620$ N/mm) and PUR ($G_c = 0.25$ N/mm and $G_f = 290.9$ N/mm), respectively. PUR was least effected by elevated temperature, and no significant differences for G_c and G_f between TR and RT bondline orientations were found for MUF and PUR treated at 20°C/65% relative humidity while comparisons between other factors varied significantly. Treatment of specimens at elevated temperatures resulted in reduced fracture performance regardless of wood grain orientation or the adhesive system.

ARTICLE HISTORY
Received 15 July 2022
Revised 3 October 2022
Accepted 9 October 2022

KEYWORDS
crack; fracture; grain orientation; temperature; European beech

Introduction

European beech (*Fagus sylvatica* L.) is currently the most widely spread hardwood species in Central Europe (Ehrhart 2019). Although a recent model shows a decline in stock and negative long-term yields in decades to come, due to severe climate change (Ehrhart 2019, Martinez del Castillo *et al*. 2022), beech could become a prospective hardwood species for structural/timber members, such as glue-laminated timber (GLT), due to its high mechanical performance, good bonding characteristics, and wide availability (Glavnić Uzelac *et al*. 2020). Adhesive joints are commonly loaded in all three modes (mode I – tension, mode II – shear, and mode III – torsion), and their combination is of concern. Mode I is regarded to be of primary importance due to its lowest fracture energy to onset cracks (River 2003). Since the fracture toughness of wood tends to be smaller in mode I than for mode II or III, the crack onset in mode I requires less energy for its initiation (Yoshihara and Kawamura 2006). To characterize fracture in mode I, one can use several tests and specimen geometries such as double cantilever beams (DCB), compact tensile tests (CT), single edge-notched three-point bending tests (SEN-TPB), or single edge-notched-tension and asymmetric four-point bending (Yoshihara 2010). The linear elastic fracture mechanics (LEFM) approach of strain energy release rate (G) and stress-intensity factor (K) are known as global energy balance and local stress distribution around the crack tip, respectively, with G standing for available energy for crack growth and K as fracture toughness (Smith *et al*. 2003). The author favors G, as it is directly measured from the energy input needed for developing a new surface, while K is more of an integration constant with high accuracy on crack tip geometry and indirect physical meaning.

Some studies conducted on beech wood followed CT test for analyzing adhesive bondlines (Watson *et al*. 2013), impacts of thermal treatment (Majano-Majano *et al*. 2012), fracture properties in relation to fractal dimensions (Hu *et al*. 2021), and methods comparison for calculation of K value (Merhar and Bučar, 2013). According to Yoshihara and Usuki (2011) K_{IC} often measured by CT test delivers material's localized parameters as a material property and provides less information than G. With a smaller effect of crack length on outputs, the DCB test was favored and recognized as the most appropriate testing approach (Yoshihara and Kawamura 2007). DCB tests were used to investigate G_I for two structural adhesives with the impact of different climate conditions (Ammann and Niemz 2015b), to develop a cohesive law for beech wood in TL plane (Gomez-Royuela *et al*. 2022), and to study the impact of wood thermal modification on fracture phenomena in mode II (Sebera *et al*. 2019). Bondline fracture of various structural adhesives in mode II was also studied by Sebera *et al*. (2020) who confirmed the application of DCB three-point bending test for characterizing adhesive bondlines on bonded beech. While Clerc *et al*. (2019) studied crack propagation in mode II under a cyclic loading regime

CONTACT Jaka Gašper Pečnik jaka.pecnik@innorenew.eu Andrej Marušič Institute, University of Primorska, Muzejski trg 2, 6000 Koper, Slovenia
Supplemental data for this article can be accessed online at https://doi.org/10.1080/17480272.2022.2135135.
This article has been corrected with minor changes. These changes do not impact the academic content of the article.

coupled with acoustic emission. On the other hand, according to the published studies adopting the SEN-TPB test, authors favor this method over DCB because (i) the crack plane direction due to orthotropic wood structure, where among six principal systems, RL and TL are adequate for DCB only (de Moura *et al*. 2010), (ii) complexity of adopting beam theory for calculating fracture toughness (Yoshihara 2010), and (iii) influence of size and dimensions for reduced material variability (de Moura *et al*. 2010, Dourado *et al*. 2015). Dourado *et al*. (2008) described that the fracture process zone (FPZ) in the SEN-TPB test is determined by specimen geometry and material characteristics, which led to more developed data reduction schemes to overcome the issues with various test setups. A data reduction scheme using compliance-based beam theory, equivalent crack length approach, and triangular-shaped stress relief region (SRR) allowed the formation of crack-resistance curve without using crack tip displacement monitoring, only by means of load–displacement diagrams and not being material sensitive (De Moura *et al*. 2010). Since the triangular shape of SRR was not fully applicable for specimens with any beam dimension and with difficulties using alternative procedures such as the bisection method, Dourado *et al*. (2011) proposed modification of the method towards the use of rectangular SRR, which enabled a direct calculation of equivalent crack length (a_{eq}) and G_I.

The effect of elevated temperature on adhesive-bondline performance has been investigated in several studies that show a general pattern – an increase in temperature typically results in decreased mechanical performance. Richter *et al*. (2006) reported the importance of the chemical composition of PUR adhesives and bondline thickness on the mechanical performance of adhesives under elevated temperatures. The impact of the chemical composition of PUR adhesives on the shear strength obtained by a lap-shear tensile test was also confirmed by Clauß *et al*. (2011) who examined various adhesives against resistance to temperatures from 20 to 220°C. For most adhesives, the study showed decent thermal stability up to 150°C, while higher temperatures resulted in greater decreases and changes in failure behavior. Study by Sedliačik and Šmidriaková (2012) found decreasing shear strength for bonded beech and spruce wood on several adhesives with increasing temperature up to 110°C as well as for spruce finger joints under bending test. Finger joints glued with four 1C-PUR adhesives and melamine-urea formaldehyde (MUF) tested at elevated temperatures were also studied by Klippel *et al*. (2011), who reported PUR systems were more affected by increasing temperature than MUF. A comprehensive study on the fracture toughness of wood and wood-based composites exposed to elevated temperatures was done by Sinha *et al*. (2012). With elevated temperature, fracture properties (steady-state strain energy release rate – G_{SS}) were also reduced, and for the laminated composites with higher resin content, an even more severe decrease was observed.

Previous findings clearly demonstrate the importance of studying and reporting the effect of elevated temperature when performing adhesive bond testing and fracture properties should be included in these studies. Accordingly, the objectives of this study were: (i) to employ SEN-TPB to characterize beech-adhesive bondline made with three different adhesives, (ii) to obtain strain energy release rate and fracture energy of adhesive bondline with selected adhesives, (iii) to evaluate the influence of bondline plane orientation (RT and TR) on fracture properties, and (iv) to evaluate the adhesive-bondline fracture performance under three different temperature regimes; 20°C, 70°C, and 140°C.

Materials and methods

For the process of bonding, two structural adhesives and one other adhesive were selected for the study: (i) a one-component poly- urethane (1C-PUR, structural) adhesive (PURBOND HB S309 type I), an adhesive for a non-brittle bond with chemical reaction during hardening and with fire resistance properties: (ii) a two-component liquid melamine-urea-formaldehyde (MUF, structural) adhesive (Prefere 4535 with 5046 hardener, a type I) for load- bearing applications and (iii) a two-component D4 emulsion-polymer isocyanate (EPI, non-structural) adhesive (Rakollit 280 and RAKOLLIT-Härter WS 1 hardener), which is an aqueous synthetic-based resin using an isocyanate compound for cross-linking. The adhesive spread rate, pressing time, and pressure used for bonding were adopted from the manufacturers' guidelines and are presented in Table 1.

Specimen preparation and conditions

Knot and crack-free boards with growth ring orientation in tangential and radial directions were cut from European beech and conditioned in a climate chamber using standard conditions (20°C/65% relative humidity (RH)) to reach 12% equilibrium moisture content. Three pairs of lamellae were selected for each group of adhesives and each wood grain orientation to manufacture glued samples for each variable. Lamellae were planed and cut to final dimensions (length × width × thickness/400 × 40 × 10 mm) prior bonding. Density was determined for all lamellae, and grouped in pairs with similar densities. A thin layer of adhesive tape of 20 mm width was applied on the longer flat-side of one lamella to introduce an area without the bondline and ensure the initial crack tip. The flat-side bonded surface of the lamellae is differentiated in two wood plane orientations by having RT and TR orientations where the first index is normal plane to crack, and the second index is the direction of crack propagation. Beams were then inserted into the press following the selected pressing regime for each adhesive (Table 1). All the samples were pressed at approx. 20°C. After bonding,

Table 1. Adhesive selection and processing conditions.

Adhesive	Spread rate (g/m^2)	Pressing time (h)	Pressure (MPa)	Mixing ratio	Viscosity (mPa s)
PUR	180	2	1	/	24,000 at (20°C)
EPI	150	2	1	100:14	10,000 at (20°C)
MUF	375	5	1	100:60	3000–3500 (25°C)

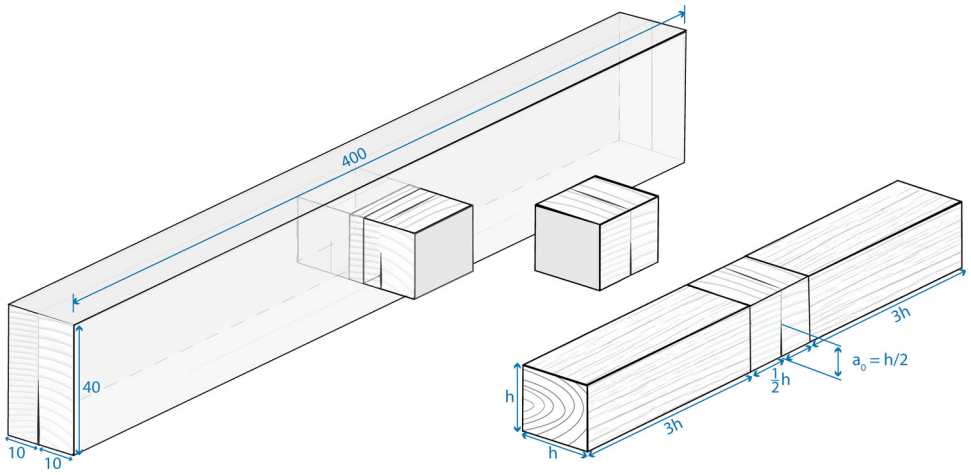

Figure 1. Manufacture of beams (dimensions in mm) and schematic presentation of wooden block cut outs with geometry proportions (h = height) for SEN-TPB test specimens.

samples were conditioned at 20°C/65% RH. Wooden blocks with dimensions of 20 × 20 mm (height × width) were cut from the beams with a targeted 10 mm bondline area and 10 mm of an unglued area over the block height. These blocks were further extended with lateral beech arms with dimensions of 60 × 20 × 20 mm (length × width × thickness) using PUR adhesive to manufacture the final specimen geometry. The proposed geometry followed the NT BUILD 422 standard (NT Build, 1993). In Figure 1, a schematic view of specimen with RT crack orientation is presented.

For each adhesive system and both wood plane orientations, 10 specimens were manufactured from each beam for a total of 30 specimens. Groups with specimens and orientations are presented in Table 2.

In addition to fracture specimens, standard lap-shear specimens were manufactured according to the EN 302-1 standard (CEN 2013) geometry to evaluate the adhesive strength and confirm the relevance of selected bonding parameters. Clean, knot-free beech lamellae were conditioned at 20°C/65% RH prior to planning and bonding. For each adhesive system, three pairs of lamellae were prepared with mixed grain orientation with a total of 18 specimens. Specimens were further conditioned until testing. The fracture specimens were randomly distributed into three groups for conditioning regimes with an even number of specimens per treatment. Specimens in the control (reference) group were conditioned at 20°C/65% RH until the testing. To assess the impact of elevated temperature on fracture properties, thermal treatments at 70°C and 140°C were held in the oven for the remaining two groups. One adhesive group at a time (20 specimens) was inserted into the preheated oven. To estimate the time to reach the target temperature, a wired thermocouple temperature was inserted into a single extra specimen to monitor its temperature. After the target temperature was reached (±3°C), the specimens stayed in the chamber for one more hour. On average, the heating phase took 30 and 60 min prior to soaking at 70°C and 140°C, respectively. Additionally, the specimen was treated to obtain the MC of the group after the heating phase.

Table 2. Crack plane orientations, adhesive system, average lamellae densities with standard deviation (SD), and number of specimens (n.).

Crack plane	Adhesive	Average lamellae density (kg/m^3)	SD (/)	n. of specimens
RT	PUR	701	14.3	30
	EPI	716	25.1	30
	MUF	680	37.9	30
TR	PUR	761	45.3	30
	EPI	731	18.6	30
	MUF	691	6.5	30

Lap shear, compression tests, and SEM

Lap-shear tests were performed on a Zwick Roell Z50 universal testing machine, using a 50 kN load cell and hydraulic grips. A testing speed of 5 mm/min was used. After specimen failure, its bonded area was measured with a caliper, and a visual estimation between wood and adhesive failure was carried out. To obtain the influence of temperature treatment on the modulus of elasticity in the longitudinal direction (E_L), compression tests parallel to the fiber (CT_{II}) were carried out using a Zwick Roell Z50 at a feeding rate of 2 mm/min. Information from CT_{II} was used as a material property of glued arms needed in the computation of equivalent crack length (a_{eq}) and flexural modulus (E_{Tf}) using the beam compliance approach for mode I. For the CT_{II} tests, two groups of nine specimens with dimensions 60 × 20 × 20 mm (height × width × thickness) were prepared. The first group of specimens provided E_L for the control group and group at 70°C since it is assumed that a temperature of 70°C does not have an impact on E_L as this temperature does not decompose the main structural polymerous constituents of the wood. Compression strain was determined as a relative change in distance between two points on the body surface recorded with an Aramis (Carl Zeiss GOM Metrology GmbH, Braunschweig, Germany) digital image correlation (DIC) system with 2 Hz data acquisition rate and camera resolution of 5 MPx. Volume and mass were determined prior to testing. After testing, the remaining specimens were dried at 103°C to determine the wood moisture content (MC) at testing. After the fracture testing, six specimens were cut into small fragments to obtain fractured images using a JEOL

JSM-IT500 scanning electron microscope (Oxford Instruments, Tokyo, Japan) operating at a low vacuum (70–80 Pa), at a working distance of 10 mm at an accelerated voltage of 15 kV.

Fracture measurements and analyses

Fracture testing was done using a Zwick Roell Z100 universal testing machine equipped with a 1 kN load cell to obtain the force–displacement response of specimens in three-point bending. The span between supports was 120 mm, and the loading speed was 3 mm/min. Tests were interrupted after reaching about zero force level. Treated specimens were tested one by one immediately after leaving the oven. After failure, the fractured area was visually estimated and the initial crack length (a_0) was measured with the caliper. SEN-TPB test was used to assess the fracture properties and develop crack–resistance curves. The selection of this geometry was guided with the aim of reducing wood anatomy impacts to obtain clearer grain orientation in the fracture area. LEFM, based on a data reduction scheme with the rectangular SRR proposed by Dourado *et al*. (2011), was used in this study. Calculation consisted of three steps. First, the flexural modulus (E_{Tf}) was calculated:

$$E_{Tf} = \left(\frac{L_2^3 - L_1^3}{bH^3} + \frac{L^3 - L_2^3}{b(H - ka_0)^3}\right) \cdot \left(\frac{C_0}{2} - \frac{L_1^3}{E_L bH^3}\right)^{-1} \quad (1)$$

where L is the half span, L_1 is the arm length from bondline to support, L_2 is the arm length shortened by SRR ($L_2 = L - ka$), b is the width of the specimen, H is the specimen height, E_L is the normal elastic modulus of arms parallel to fiber, a_0 is the initial crack length, C_0 is the initial compliance, and k is the non-dimensional parameter equal to 0.9. For smaller cross-sections, where higher compressive stresses occur due to bending, the k factor needs to be higher and closer to 1, which would define square SRR. Once the E_{Tf} is obtained and used instead of E_T, equivalent crack length (a_{eq}) can be computed:

$$a_{eq} = \frac{1}{k}\left\{H - \left[\left(\frac{C}{2} - \frac{L_1^3}{ELbH^3} - \frac{L_2^3 - L_1^3}{E_{Tf}bH^3}\right)^{-1} \cdot \frac{L^3 - L_2^3}{E_{Tf}b}\right]^{\frac{1}{3}}\right\} \quad (2)$$

where C is the current compliance. Utilizing Irwin–Kies solution, direct computation of strain energy release rate (G_I) was obtained by:

$$G_1 = \frac{3P^2}{b^2}\frac{(L^3 - L_2^3)k}{E_{Tf}(H - ka_{eq})^{4'}} \quad (3)$$

where P is the force. Subsequently, from the G_I, the critical value of G_{cI} was obtained at maximal force P_{max}. Total fracture energy (G_f) was calculated as the area under the curve P vs. deflection. All fracture calculations were made using Matlab R2021b (Mathworks Inc). Average Force–displacement curves were made as an arithmetic mean of the group till the end of the shortest group data set and using the linear interpolation function interp1 available in Matlab package.

Statistical analysis

Fracture energy (G_f) and critical fracture energy (G_c) were analyzed to determine if and how wood grain orientation at bonded surfaces, adhesive or treatment temperature affected them. Linear models (LM) were fitted to log-transformed G_c and G_f as dependent variables (Suppl. Table 1, Suppl. Table 2). In each model, the independent variables were adhesives, orientation, and treatment. Individual factor effects and all two-way interactions were included in both models. Once transformed, the data met the assumptions of ordinary least squares regression. Due to the transformed dependent variables, analytical results are presented as medians on the untransformed scale with 95% confidence intervals (CI), and comparisons (contrasts) between levels of the variables are ratios between the medians of those levels when other variables are held constant. For example, comparing G_c between control specimens bonded in the TR plane, using two adhesive systems – e.g. EPI and MUF – would be reported as the ratio between the median G_c of the sample group with EPI and the sample group with MUF with a 95% CI of the ratio. *P*-values are omitted, but CI of comparisons that do not include one (1) are considered statistically significant. CI were adjusted using Tukey's method for comparing a family of three estimates. Only results of interest are presented in the paper; full results are available in supplemental tables. Tukey's HSD test was used to test for differences in the results of the lap-shear and compression tests. Effect sizes from these tests are reported as differences between estimated mean values with 95% CIs. Data analysis was conducted in R (version 4.2) using RStudio (version 2022.02.03). Comparisons between factors were calculated as marginal means using the emmeans package (Lenth 2022). The data and analytical code that support the findings of this study are available on Zenodo at https://doi.org/10.5281/zenodo.7143370.

Results and discussion

Lap-shear and compression tests

Results of the lap-shear test are presented in Table 3. The highest lap-shear strength was obtained for MUF adhesive with the lowest number of adhesive failures. In contrast, PUR adhesive group showed a 12.4% lower strength and also had the highest number of adhesive failures. Tukey's HSD test showed a significant difference in strength only

Table 3. Results of lap-shear tests for different adhesives, with number of tested specimens (*n*), average lamellae densities with standard deviation (SD), average strength, overall percentage of adhesive area failure, and number (*n*.) of failed specimens in adhesive bondline.

Adhesive	*n*.	Density (kg/m^3)	SD (/)	Strength (MPa)	SD (/)	Adhesive failure area (%)	Adhesive failure (*n*.)
PUR	18	700	41.01	14.8	1.9	50–100	18
EPI	18	730	32.2	16.2	3.1	10–50	7
MUF	17	732	47.3	16.9	1.9	40	1

between MUF and PUR adhesive groups (MUF-PUR: 2.02 MPa, 95% CI: 0.09–3.96 MPa, $p = 0.038$). Nevertheless, bonding strengths of all adhesives surpassed a threshold strength of 10 MPa according to EN 302-1, A1 class for standardized climate conditions.

Clauß *et al*. (2011) reported slightly lower values for glued beech; 12.7 and 12.3 MPa for EPI and MUF, respectively, and between 12.1 MPa to 13.4 MPa for different PUR adhesive systems. Bachtiar *et al*. (2017) reported values of 13.4 and 12.9 MPa for PUR and MUF, respectively. The reported studies followed the wood grain angle between 30° and 90° but in the present study, the entire orientation range with radial and tangential (0°–90°) was tested. According to Hass *et al*. (2009), grain orientation in terms of bondline shear strength showed to be an important factor. Finally, all above-mentioned studies observed a lower percentage of wood failure for PUR adhesives compared to other adhesives. Nevertheless, in this study, lap-shear experiments were conducted only to confirm the quality of the selected bonding process.

Control specimens for compression tests were tested with an average MC of 10%, while treated specimens at 140°C reached MC below 1%. For the control group, the average density was 706 kg/m^3, and the average E_L was 14.6 GPa (SD = 3.7); for the specimens treated at the elevated temperature (140°C), the average density and E_L were found 655 kg/m^3 and 13.6 GPa (SD = 2.8), respectively. Tukey's HSD test suggested no significant difference between the two groups ($p = 0.53$); therefore, testing of specimens with elevated temperature treated at 70°C was skipped. Results for the control group are comparable with the existing reported literature below and it was expected that stiffness would increase for thermally treated specimens due to MC reduction (Kollmann and Côté 1968, Ozyhar *et al*. 2013, Straže *et al*. 2016). Hering *et al*. (2012) reported 13.9 GPa for E_L in CT_{II} measured by crosshead for beech wood with a density of 691 kg/m^3 and 12% MC. Measurements of local deformation on the surface of the specimens using DIC provide more precise and reliable strain data than a global measuring system based on reading displacement from the test machine. Gomez-Royuela *et al*. (2021) employed DIC for strain measurement in CT_{II} test and obtained E_L of 13.8 GPa for beech with a density of 677 kg/m^3 and 12% MC. Further, Ozyhar *et al*. (2013) obtained E_L of 11 and 12.9 GPa for beech wood of 0% and 11% MC, respectively. However, none of the mentioned studies were conducted on the heated specimens. Visco-elasticity becomes more pronounced with a combination of heat and moisture which plasticize and soften the wood (Sandberg *et al*. 2021). Values of E_L obtained in the study were used for further calculations of fracture characteristics.

Fracture test and analyses

The fracture tests consisted of a series of SEN-TPB tests that resulted in force-displacement (F/δ) data sets for each adhesive and temperature (Figure 2). As is demonstrated in Figure 2, the maximal force (F_{max}) reached differs from adhesive to adhesive; however, all adhesives reveal the same pattern with respect to the effect of the temperature. As the temperature increases, F_{max} decreases significantly. The smallest decrease of F_{max} due to raised temperature is for the PUR adhesive. For the control and 70°C treatment groups, the highest rate of wood fracture was found for MUF in TR orientation, where most of the specimens fractured in the wood-adhesive interface (from 70 to 100% of fractured area). Fiber bridging in wood-adhesive interface failures resulted in a slower and longer decline in force after F_{max} was reached. Typically, the crack was initiated at the tip of the adhesive line and then propagated along the interface parallel to the bondline. In RT orientation, the majority of cracks propagated in the adhesive with specimens ranging between 30 and 50% wood fracture area. Similar observations were obtained for EPI in TR orientation but with a lower percentage of fractured area in wood (ranging from 40 to 90%). For the few cases within this group, crack propagated away from the bondline direction, i.e. in the direction of the wooden rays which ended up in slightly higher F_{max}

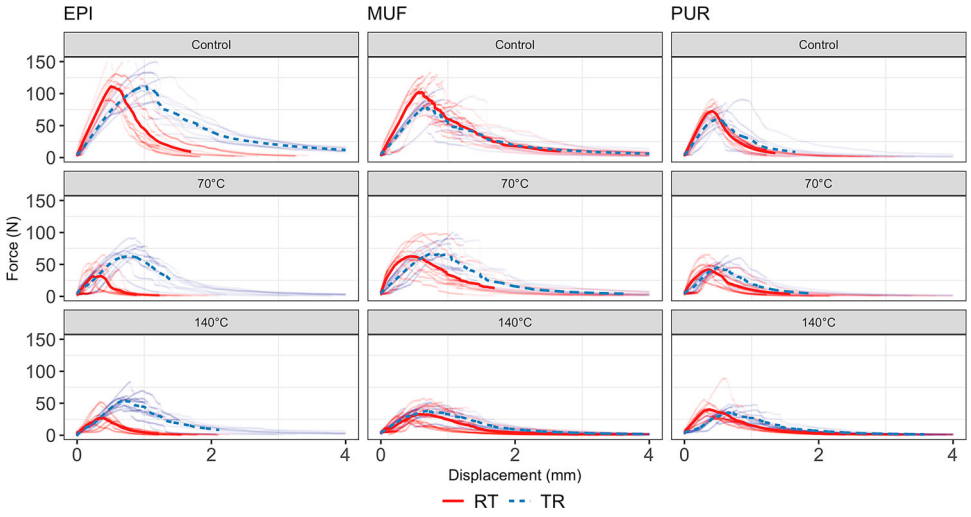

Figure 2. Force–displacement diagrams for each group of adhesives with different treatments. Average curves are presented with bold and dashed lines for RT and TR planes.

compared to those fractured in the bondline. Such cases are likely due to the variability of wood properties, which results in highly complex crack paths in the wood and around the bondline. On the other hand, EPI in RT orientation and PUR in both orientations resulted in pure adhesive (bondline) fracture with little or no fiber bridging in the wood-adhesive interface. For the 140°C group, MUF and EPI with TR orientation also exhibited an overall wood fracture area ranging from 50 to 100% failure. In RT orientation, all the adhesive groups fractured purely within the adhesive; only a few MUF specimens fractured in the wood-adhesive interface.

In Figure 2, bold lines represent the average curves of F/δ diagrams. In most cases, except for the MUF group at 140°C, the RT orientation resulted in higher initial stiffness. Conversely, it could be observed that after F_{max} was reached, the curves in groups with the RT bonding dropped more abruptly and in a more brittle manner. These findings can be attributed to the (i) impact of bonding direction and its influence on the adhesive penetration; (ii) adhesive system; (iii) difference in expected surface topography for the TR and RT planes, and (iv) MC of tested specimens. Not just orientation but also temperature treatment impacts the general curve shape. Regardless of the plane orientation for the control groups, a rather sharp decline in force was notable after reaching F_{max}. While on the other hand, temperature-treated groups reduced the brittle-like failures with a more steady force reduction. Such behavior can be argued with reduced fracture properties of wood material in the case of wood-adhesive fracturing, impact of moisture, and impact of temperature on the material properties, i.e. softening. MC for tested specimens was on average 7% and below 1% for 70°C and 140°C temperature treatment, respectively.

Reiterer (2001) observed the largest decrease in specific G_I when testing beech in the RL fracture plane from 60°C to 80°C. Changes in fracture parameters due to elevated temperature on solid wood were also reported for birch and spruce by Tukiainen and Hughes (2016) and Dourado and Moura (2019). On the other hand, Ammann and Niemz (2015b) reported higher G_I for PRF bondlines on beech wood when specimens showed 12% and 15% MC rather than 21%, but no such influence was found for PUR bondline. It was also noted that composites with higher resin loading showed a larger decrease in G_{SS} as temperature may deteriorate resins' capacity (Sinha *et al.* 2012).

Using Equations (1–3) resulted in relationships between strain energy release rate (G_I) and equivalent crack length (a_{eqv}), as shown in Figure 3. For better clarity, Figure 3 shows only data slightly after reaching the critical value of G at F_{max} (G_c), so the effect of fiber bridging is visible only on F/δ diagrams.

In general, Figure 3 shows that all of the groups have a certain plateau for stable crack growth after reaching G_c, even though the data reveal high variability and noise at low values of G due to computational reasons at low forces and displacements. The variability of G progression might be lowered using even smaller loading speed than in our case (3 mm/min). It should be noted that G_c decreases as the temperature of treatment rises.

SEM studies of fractured surfaces for selected control specimens with the inserted images of the fractured specimens are presented in Figure 4. As it can be seen from these images, MUF and EPI with TR orientation are showing typical wood failure (Figure 4(c,e)) while PUR resulted in adhesive failure (Figure 4(a)). In the RT orientation, wood failure occurred only in the case of MUF adhesives, while adhesive failure occurred in the case of EPI and PUR adhesives (white arrows in Figure 4). There are several factors affecting bond properties like, i.e. gluing process, adhesive system, and wood (Gavrilović-Grmuša *et al.* 2012, Sterley 2012). It is well known that adhesives with high viscosity have low penetration ability into the wood; a thick interface results in a large portion of wood failure compared to a thin interface (Gavrilović-Grmuša *et al.* 2012). Low viscosity and a high amount of adhesive can explain the higher proportion of wood failure in MUF compared to the other two adhesives. It was reported that the penetration depth for European beech in the tangential direction is greater than in the radial direction (Sernek *et al.* 1999) while others indicate no major differences in penetration depth between radial and tangential directions (Gavrilović-Grmuša *et al.* 2012). Similar mechanisms of fractured

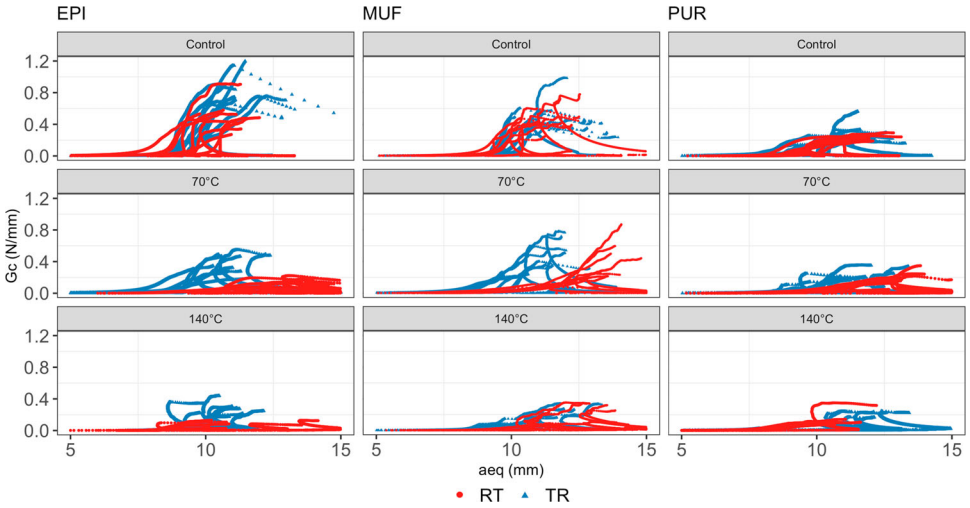

Figure 3. Strain–energy release rate vs. equivalent crack length at examined temperature for all adhesives.

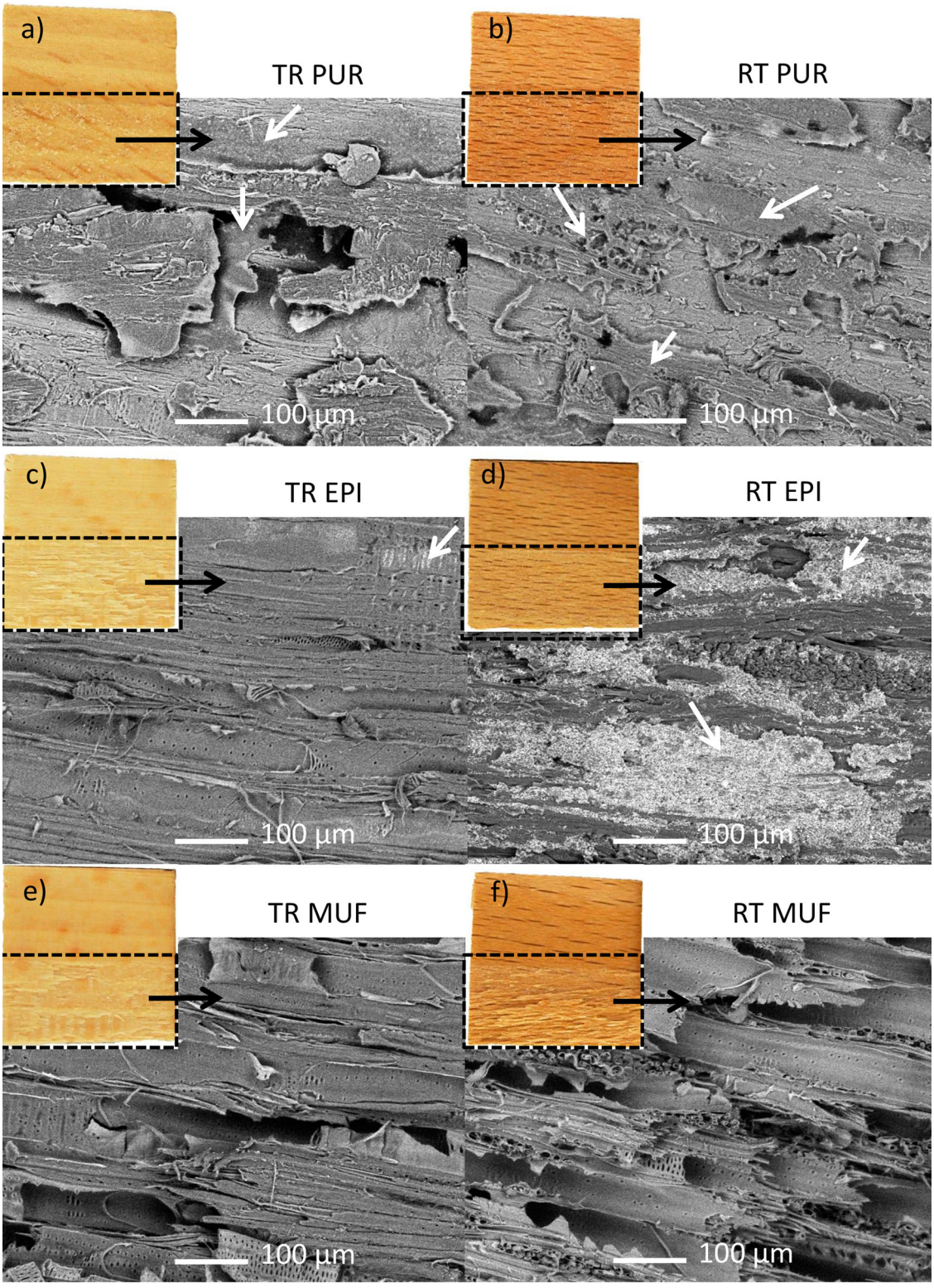

Figure 4. SEM images of the fractured surfaces for selected control specimens for TR and RT plane orientation for (a,b) PUR, (c,d) EPI, and (e,f) MUF. Wooden inlays are fractured bondline images for each representative specimen after the fracture test (the marked dotted area is the observed, glued area). White arrows indicate the adhesive residues.

adhesive joint failures for PUR and MUF were reported also by Watson *et al.* (2013) and for PUR by Ammann *et al.* (2015a, 2015b). In addition, cured PUR adhesive on the surface was identical to that reported by Richter *et al.* (2006), who also reported an excess of bubbles for the CO_2 release during the curing which is closely related to a high failure rate in case of a thick bondline.

Experimentally observed results for G_c, G_f with average, standard deviation, and median values are presented in Table 4.

Table 4. Number of analyzed specimens, observed average values with standard deviation (SD), and median results (med) of G_c and G_f for adhesive groups, TR and RT orientation and temperature level of the temperature treatment.

	TR			RT		
	PUR	EPI	MUF	PUR	EPI	MUF
Control						
Count	10	10	10	10	10	10
G_c (N/mm)	0.25	0.80	0.50	0.19	0.45	0.47
SD	0.11	0.20	0.16	0.04	0.17	0.16
G_c – med (N/mm)	0.24	0.71	0.45	0.19	0.45	0.43
G_f (N/mm)	290.9	1079.4	620.0	246.9	485.2	617.2
SD	122.1	197.2	195.9	34.6	200.8	145.6
G_f – med (N/mm)	266.6	1090.5	652.3	245.4	438.3	578.7
70°C						
Count	9	10	10	10	10	10
G_c (N/mm)	0.21	0.34	0.44	0.16	0.13	0.31
SD	0.08	0.12	0.12	0.08	0.05	0.22
G_c – med (N/mm)	0.19	0.36	0.43	0.15	0.12	0.24
G_f (N/mm)	218.3	407.2	509.9	171.2	83.4	401.7
SD	61.3	107.1	151.8	58.6	27.0	219.6
G_f – med (N/mm)	211.0	395.4	448.3	174.1	73.1	335.3
140°C						
Count	8	10	10	8	7	10
G_c (N/mm)	0.18	0.27	0.19	0.18	0.08	0.18
SD	0.07	0.08	0.10	0.09	0.04	0.12
G_c – med (N/mm)	0.19	0.27	0.20	0.09	0.08	0.18
G_f (N/mm)	224.7	367.3	290.9	192.8	90.3	204.9
SD	65.6	99.7	80.5	64.6	42.8	109.4
G_f – med (N/mm)	194.6	357.7	309.4	183.6	88.9	199.7

For the control group (20°C/ 65% RH), the lowest G_c and G_f values were found for RT bondline, and the temperature increase intensified this trend. In the control group, PUR adhesive showed the lowest average for G_c and G_f in TR (0.25 and 290.9 N/mm) and RT plane (0.19 and 246.9 N/mm), respectively.

For MUF and EPI, this relation is less clear. The highest G_c and G_f were found for EPI control in TR plane (0.80 and 1079.4 N/mm), but closer more similar results between MUF and EPI were observed in RT plane. Treatment at 70°C had a lower impact on fracture properties for the MUF adhesive with 0.44 and 509.9 N/mm in TR plane and 0.31 N/mm and 401.7 in RT plane for G_c and G_f, respectively. Finally, EPI was found to maintain the highest G_c and G_f values at a temperature treatment of 140°C in TR plane. Similarly, this was observed for MUF in RT plane. Estimating the average area under the curve in Figure 2, fracture propagation in the PUR group was more rapid and of higher intensity compared to the other two adhesives, resulting in lower G_f values for the latter. The effect of thermal treatment was observed to have an impact on G_c and G_f values, resulting in lower values with increasing temperature treatment. G_c and G_f for EPI obtained the highest measures at 140°C treatment in a TR plane. For MUF, the crack orientation did not seem to have a strong impact even at elevated temperatures. Further, PUR remain with poor performance in both TR and RT bondline orientation, regardless of the temperature treatment. Treatment at 140°C was severe for few specimens; therefore, experiments were not able to analyze.

Analytical results

The LM of G_c and G_f revealed the complex relationship between bondline grain orientation, treatment temperature, and adhesive system. Performance is presented as the median estimated value for G_c or G_f with a 95% confidence interval for that estimate. When comparisons are made between groups, the estimated difference is the ratio between the medians of the compared groups, with a 95% confidence interval of the ratio. The estimated performance of each group (in terms of G_c and G_f, with greater values indicating better performance) varied based on the specific combinations of the investigated factors. That is, no treatment, adhesive, or orientation performed best in all cases. It was clear that increasing treatment temperature had a negative impact on G_c and G_f, but that effect was not consistent between adhesives. Likewise, the effect of grain orientation on G_c and G_f was more pronounced with EPI, but in the TR plane median, G_f was between 2 and 3 times greater than the RT plane. For MUF and PUR, the effect was smaller, and only at 70°C and 140°C treatment; the control group of MUF and PUR performed approximately the same in TR and RT planes. Figure 5 shows predicted medians values for G_c (Figure 5(a)) and G_f (Figure 5(b)) with 95% CI. Treatment combinations are presented in ascending order from the smallest to largest median (see Suppl. Table 3). The most apparent observations from Figure 5 are that for both G_c and G_f, TR plane under control conditions using EPI performed better than all other combinations and the least performant combinations all had RT plane. Multiple R^2 for the LMs were 0.62 and 0.79 for G_c and G_f, respectively.

Treatment temperature had a significant but inconsistent effect on performance in most cases, as shown in the following analysis for each temperature group.

Control group

Under control conditions, bondline grain orientation had no discernible impact on the control group for either PUR or MUF adhesives. In contrast, the median G_c of specimens with EPI was 2.09 times greater in the TR plane than in the RT plane (95% CI: 1.52–2.89; See Suppl. Table 4). In the TR plane, control specimens with EPI adhesive also had the highest estimated G_c, 0.84 N/mm (95% CI: 0.64–1.09; Figure 5(a)). This pattern was similar for G_f, with EPI in the TR plane outperforming EPI in the RT plane by a factor of 2.82 (95% CI: 2.24–3.54) while having the greatest predicted median G_f (1165 N/mm, 95% CI: 963.2–1409; Figure 5(b), Suppl. Table 3). Analyses revealed that for G_c under control conditions, only EPI and MUF in RT plane orientation performed similarly while others varied significantly (See Suppl. Table 4). The median G_c of EPI was 1.78 times greater (95% CI: 1.18–2.71) than MUF in the RT plane orientation, with the highest estimated G_c in this treatment (0.84 N/mm with 95% CI: 0.64–1.09; Suppl. Table 3). On the other hand, in RT plane, MUF produced the highest estimated G_c (0.46 N/mm with 95% CI: 0.35–0.60; Suppl. Table 3). For G_f, all adhesives resulted in significantly different values with a similar trend.

Treatment at 70°C

When specimens were treated at 70°C, EPI no longer performed substantially better than other adhesives but was most significantly affected by bondline grain orientation (Suppl. Table 4). Under this treatment condition, the

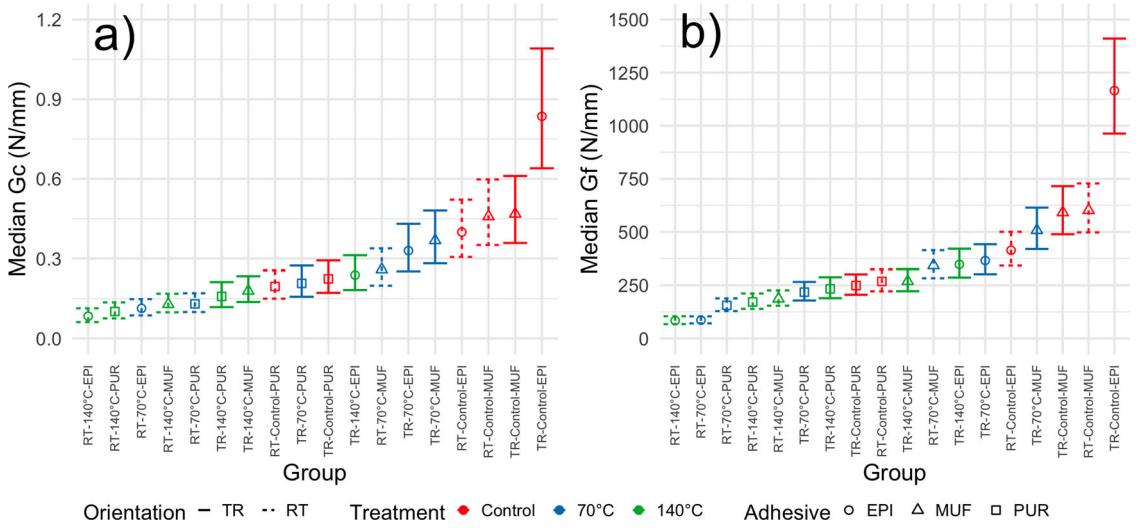

Figure 5. Estimated median (points) G_c (a) and G_f (b) of each group in ascending order with estimated 95% CI (error bars).

highest G_c and G_f were found for MUF in both bondline orientations. At a 70°C treatment temperature, orientation impacted the performance of G_c for all adhesive systems. The effect was most pronounced for EPI, where G_c in the TR plane orientation was 2.91 times (95% CI: 2.11–4.01) greater than in the RT plane orientation. Although the effect of orientation was lower for MUF, when oriented in the TR plane, MUF had the greatest estimated median G_c (0.37 N/mm, and 95% CI: 0.28–0.48; Suppl. Table 3) within the group treated at 70°C. The effect on G_f for EPI was found to be even larger than its G_c counterpart, being 4.25 times (CI: 3.38–5.35) greater in TR than RT plane, with estimated median values of 366 N/mm (95% CI: 302–442) and 86 N/mm (95% CI: 71–104), respectively (Figure 5(b); Suppl. Table 3). When treated at 70°C, group with EPI adhesive performed better than those with PUR in TR plane for both G_c and G_f. However, while there was no discernible difference between EPI and MUF in TR plane for G_c, there was a small reduction in performance for G_f (0.72 times reduction, 95% CI: 0.53–0.97). In RT plane, EPI performed worse than MUF and PUR in G_f and worse than MUF in G_c, with no evidence of a difference in G_c between EPI and PUR. MUF performed approximately two times better than PUR in both TR and RT plane orientation for both G_c and G_f (Suppl. Table 4).

Treatment at 140°C

Treatment at 140°C was found to have the most severe impact overall. No significant differences in G_c were found among adhesives in this treatment. Median G_c and G_f were found to be significantly different for all adhesive system at 140°C between TR and RT plane (See Suppl. Table 4). EPI experienced the largest change between bondline grain orientations for G_c, with TR plane predicted to be 2.85 times greater (95% CI: 2.03–4.00) than RT plane. The effect was even more pronounced for G_f, with TR plane predicted to

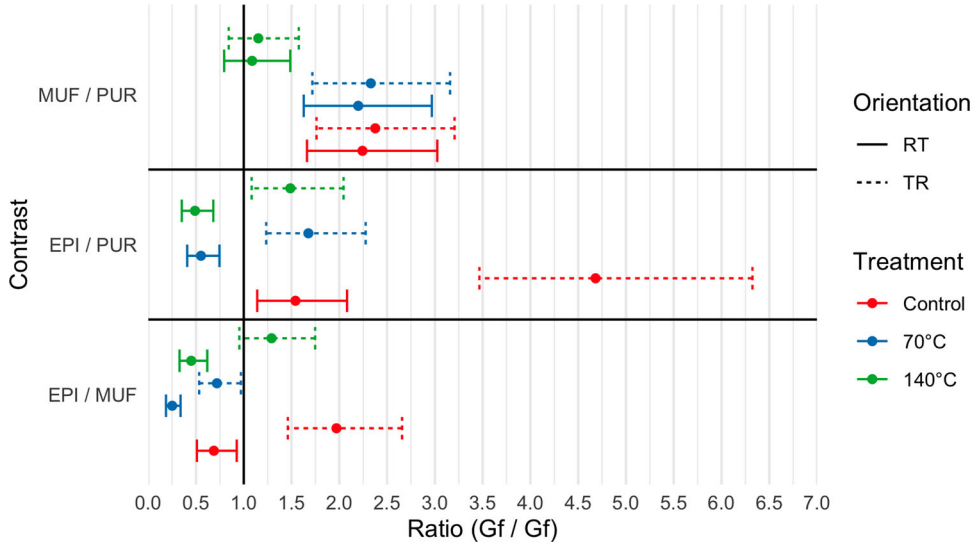

Figure 6. Ratios between the median G_f (points) of each group with estimated 95% CI (error bars), with solid or dashed lines representing the radial or tangential plane, respectively. Error bars that include ratio = 1 are not considered significantly different.

be 4.13 (95% CI: 3.24–5.26) times greater than in the RT plane. EPI in TR plane at 140°C treatment temperature was predicted to have the highest G_f (347.4 N/mm, 95% CI: 286.5–421.2; Suppl. Table 3) while the same combination with RT plane in the 140°C temperature group was the predicted to be the lowest (84.1 N/mm, 95% CI: 67.6–104.6). Surprisingly, these values are nearly identical to the predicted values for the same factor combinations at a treatment temperature of 70°C (Suppl. Table 3), indicating that while heat treatment does have an impact on EPI performance, it does not seem to change based on the treatment temperatures tested in this study. The dominant effect for EPI is clearly bondline grain orientation.

Comparison between treatments

Figure 6 shows an overview of the comparison for G_f between adhesives, for each temperature and orientation. More interesting is that EPI and PUR resulted in no significant differences in G_c between the two treatments for both orientations, while MUF experienced a more severe impact at this treatment level with 2.06 (95% CI: 1.35–3.13) and 2.01 (95% CI: 1.32–3.07) greater reductions from 70°C treatment in TR and RT plane orientation, respectively. G_f values were least impacted by PUR adhesive. Comparing G_c between the control and 140°C treatment groups, the most severe decreases were observed for EPI in RT plane with 4.77 (95% CI: 3.06–7.45) and 3.50 (95% CI: 2.29 −5.36) greater reductions with RT and TR plane orientations, respectively.

Conclusion

In this paper, the adhesive-bondline fracture behavior of three structural adhesives on European beech wood was analyzed at three different temperature treatments and with two wood grain orientations with respect to the crack plane (TR and RT). Fracture energy and critical strain energy release rate were obtained from the SEN-TPB test in mode I. Regarding the fracture performance of the adhesive bondlines PUR, in general, performed the worst among all adhesives in terms of G_c and G_f, although it was the least impacted by elevated temperature treatment. Conversely, EPI reached the highest observed G_c and G_f values when tested at standard conditions but experienced the most severe decrease in fracture properties when tested after treatment at an elevated temperature. EPI in all treatment groups showed the most significant change in properties related to crack plane orientation, which was less pronounced for the other two adhesives (MUF and PUR). In general, the study showed that SEN-TPB test employing data reduction scheme may be advantageous for fracture analysis of adhesive bonds and that the impact of temperature on adhesive-bondline performance is significant when EPI, MUF, and PUR are used. As the examined treatment temperatures were lower than the decomposition temperature of wood's main components, it is clear that adhesive-bondline characteristics (grain orientation, adhesive) should be selected carefully in applications where the elevated temperature might occur.

Disclosure statement

No potential conflict of interest was reported by the author(s).

Funding

This work has been conducted with the financial support of the European Commission for the InnoRenew project [Grant Agreement #739574] under the Horizon2020 Widespread-2-Teaming program, Republic of Slovenia (Investment funding of the Republic of Slovenia and the European Union of the European Regional Development Fund), Slovenian Research Agency (infrastructure program IO-0035) and Slovenian Research Agency (basic research funding No. P4-0430). The authors also acknowledge the grant provided by Czech Science Foundation: "Experimental and numerical assessment of the bearing capacity of notches in timber beams at arbitrary locations using LEFM" (#21-29389S).

ORCID

Jaka Gašper Pečnik http://orcid.org/0000-0002-8775-8230
Andreja Pondelak http://orcid.org/0000-0003-1078-389X
Michael David Burnard http://orcid.org/0000-0001-9357-0819
Václav Sebera http://orcid.org/0000-0002-2658-1179

References

Ammann, S. and Niemz, P. (2015a) Mixed-mode fracture toughness of bond lines of PRF and PUR adhesives in European beech wood. *Holzforschung*, 69(4), 415–420.

Ammann, S. and Niemz, P. (2015b) Specific fracture energy at glue joints in European beech wood. *International Journal of Adhesion and Adhesives*, 60, 47–53.

Bachtiar, E. V., Clerc, G., Brunner, A. J., Kaliske, M. and Niemz, P. (2017) Static and dynamic tensile shear test of glued lap wooden joint with four different types of adhesives. *Holzforschung*, 71(5), 391–396.

CEN (2013) *BS EN 302-1. Adhesives for Load-Bearing Timber Structures – Test Methods* (Brussels, Belgium).

Clauß, S., Joscak, M. and Niemz, P. (2011) Thermal stability of glued wood joints measured by shear tests. *European Journal of Wood and Wood Products*, 69(1), 101–111.

Clerc, G., Brunner, A. J., Josset, S., Niemz, P., Pichelin, F. and Van de Kuilen, J. W. G. (2019) Adhesive wood joints under quasi-static and cyclic fatigue fracture mode II loads. *International Journal of Fatigue*, 123 (February), 40–52.

de Moura, M. F. S. F., Dourado, N. and Morais, J. (2010) Crack equivalent based method applied to wood fracture characterization using the single edge notched-three point bending test. *Engineering Fracture Mechanics*, 77(3), 510–520.

Dourado, N. and de Moura, M. F. S. F. (2019) Effect of temperature on the fracture toughness of wood under mode I quasi-static loading. *Construction and Building Materials*, 223, 863–869.

Dourado, N., De Moura, M. F. S. F. and Morais, J. (2011) A numerical study on the SEN-TPB test applied to mode i wood fracture characterization. *International Journal of Solids and Structures*, 48(2), 234–242.

Dourado, N., de Moura, M. F. S. F., Morel, S. and Morais, J. (2015) Wood fracture characterization under mode I loading using the three-point-bending test. Experimental investigation of *Picea abies* L. *International Journal of Fracture*, 194(1), 1–9.

Dourado, N., Morel, S., de Moura, M. F. S. F., Valentin, G. and Morais, J. (2008) Comparison of fracture properties of two wood species through cohesive crack simulations. *Composites Part A: Applied Science and Manufacturing*, 39(2), 415–427.

Ehrhart, T. (2019) European beech glued laminated timber. Thesis (PhD). ETH Zürich.

Gavrilović-Grmuša, I., Dunky, M., Miljković, J. and Djiporović-Momčilović, M. (2012) Influence of the degree of condensation of urea-formaldehyde adhesives on the tangential penetration into beech and fir and on the shear strength of the adhesive joints. *European Journal of Wood and Wood Products*, 70(5), 655–665.

Glavnić Uzelac, I., Boko, I., Torić, N. and Vranković Lovrić, J. (2020) Application of hardwood for glued laminated timber in Europe subject. *Gradjevinar*, 72(7), 607–616.

Gómez-Royuela, J. L., Majano-Majano, A., José Lara-Bocanegra, A. and Reynolds, T. P. S. (2021) Determination of the elastic constants of thermally modified beech by ultrasound and static tests coupled with 3D digital image correlation. *Construction and Building Materials*, 302, 124270.

Gómez-Royuela, J. L., Majano-Majano, A., Lara-Bocanegra, A. J., Xavier, J. and de Moura, M. F. S. F. (2022) Evaluation of R-curves and cohesive law in mode I of European beech. *Theoretical and Applied Fracture Mechanics*, 118, 1–9.

Hass, P., Müller, C., Clauss, S. and Niemz, P. (2009) Influence of growth ring angle, adhesive system and viscosity on the shear strength of adhesive bonds. *Wood Material Science and Engineering*, 4(3–4), 140–146.

Hering, S., Keunecke, D. and Niemz, P. (2012) Moisture-dependent orthotropic elasticity of beech wood. *Wood Science and Technology*, 46(5), 927–938.

Hu, W., Liu, Y. and Li, S. (2021) Characterizing mode I fracture behaviors of wood using compact tension in selected system crack propagation. *Forests*, 12(10), 1–13.

Klippel, M., Frangi, A. and Fontana, M. (2011) Influence of the adhesive on the load-carrying capacity of glued laminated timber members in fire. *Fire Safety Science*, 10, 1219–1232.

Kollmann, F. F. P. and Côté, W. A. (1968) *Principles of Wood Science and Technology I Solid Wood* (Berlin: Springer).

Lenth, V. R. (2022) emmeans: Estimated Marginal Means, aka Least-Squares Means.

Majano-Majano, A., Hughes, M. and Fernandez-Cabo, J. L. (2012) The fracture toughness and properties of thermally modified beech and ash at different moisture contents. *Wood Science and Technology*, 46(1–3), 5–21.

Martinez del Castillo, E., Zang, C. S., Buras, A., Hacket-Pain, A., Esper, J., Serrano-Notivoli, R., Hartl, C., Weigel, R., Klesse, S., Resco de Dios, V., Scharnweber, T., Dorado-Liñán, I., van der Maaten-Theunissen, M., van der Maaten, E., Jump, A., Mikac, S., Banzragch, B. E., Beck, W., Cavin, L., Claessens, H., Čada, V., Čufar, K., Dulamsuren, C., Gričar, J., Gil-Pelegrín, E., Janda, P., Kazimirovic, M., Kreyling, J., Latte, N., Leuschner, C., Longares, L. A., Menzel, A., Merela, M., Motta, R., Muffler, L., Nola, P., Petritan, A. M., Petritan, I. C., Prislan, P., Rubio-Cuadrado, Á, Rydval, M., Stajić, B., Svoboda, M., Toromani, E., Trotsiuk, V., Wilmking, M., Zlatanov, T. and de Luis, M. (2022) Climate-change-driven growth decline of European beech forests. *Communications Biology*, 5(1), 1–9.

Merhar, M., Bučar, D. G. and Bučar, B. (2013) Faktor kritičnog intenziteta naprezanja (i. mod) bukovine (*Fagus sylvatica*) u TL presjeku: Usporedba različitih metoda. *Drvna Industrija*, 64(3), 221–229.

NT BUILD 422 (1993) Wood: Fracture energy in tension perpendicular to the grain. Nordtest Method, 11. Tekniikantie, Finland.

Ozyhar, T., Hering, S. and Niemz, P. (2013) Moisture-dependent orthotropic tensioncompression asymmetry of wood. *Holzforschung*, 67(4), 395–404.

Reiterer, A. (2001) The influence of temperature on the mode I fracture behavior of wood. *Journal of Materials Science Letters*, 20(20), 1905–1907.

Richter, K., Pizzi, A. and Despres, A. (2006) Thermal stability of structural one-component polyurethane adhesives for wood-structure-property relationship. *Journal of Applied Polymer Science*, 102(6), 5698–5707.

River, B. (2003) Fracture of adhesive-bonded wood joints. In A. Pizzi and K. L. Mittal (eds.), *Handbook of Adhesive Technology, Revised and Expanded* (2nd ed.). (New York: Marcel Dekker. Inc., 325–350).

Sandberg, D., Kutnar, A., Karlsson, O. and Jones, D. (2021) *Wood Modification Technologies: Principles, Sustainability, and the Need for Innovation* (1st ed.) (London: CRC Press).

Sebera, V., Pečnik, J. G., Azinović, B. and Huć, S. (2020) Wood-adhesive bond loaded in mode II : experimental and numerical analysis using elasto-plastic and fracture mechanics models, 5957, 1–13.

Sebera, V., Redón-Santafé, M., Brabec, M., Děcký, D., Čermák, P., Tippner, J. and Milch, J. (2019) Thermally modified (TM) beech wood: Compression properties, fracture toughness and cohesive law in mode II obtained from the three-point end-notched flexure (3ENF) test. *Holzforschung*, 73(7), 663–672.

Sedliačik, J. and Šmidriaková, M. (2012) Heat resistance of adhesive joints for wood constructions. *Acta Facultatis Xylologiae Zvolen*, 54 (2), 79–94.

Sernek, M., Resnik, J. and Kamke, F. A. (1999) Penetration of liquid urea-formaldehyde adhesive into beech wood. *Wood and Fiber Science*, 31(1), 41–48.

Sinha, A., Nairn, J. A. and Gupta, R. (2012) The effect of elevated temperature exposure on the fracture toughness of solid wood and structural wood composites. *Wood Science and Technology*, 46(6), 1127–1149.

Smith, I., Landis, E. and Gong, M. (2003) *Fracture and Fatigue in Wood* (New York: John Wiley & Sons. Inc).

Sterley, M. (2012) Characterisation of green-glued wood adhesive bonds. Thesis (PhD). Linnaeus University.

Straže, A., Fajdiga, G., Pervan, S. and Gorišek, Ž (2016) Hygro-mechanical behavior of thermally treated beech subjected to compression loads. *Construction and Building Materials*, 113, 28–33.

Tukiainen, P. and Hughes, M. (2016) The effect of temperature and moisture content on the fracture behaviour of spruce and birch. *Holzforschung*, 70(4), 369–376.

Watson, P., Clauss, S., Ammann, S. and Niemz, P. (2013) Fracture properties of adhesive joints under mechanical stresses. *Wood Research*, 58 (1), 43–56.

Yoshihara, H. (2010) Examination of the mode I critical stress intensity factor of wood obtained by single-edge-notched bending test. *Holzforschung*, 64(4), 501–509.

Yoshihara, H. and Kawamura, T. (2006) Mode I fracture toughness estimation of wood by DCB test. *Composites Part A: Applied Science and Manufacturing*, 37(11), 2105–2113.

Yoshihara, H. and Kawamura, T. (2007) Influence of the measurement methods on the mode I fracture toughness of wood. *Zairyo/Journal of the Society of Materials Science, Japan*, 56(4), 311–315.

Yoshihara, H. and Usuki, A. (2011) Mode I critical stress intensity factor of wood and medium-density fiberboard measured by compact tension test. *Holzforschung*, 65(5), 729–735.